

Contribution of the Wizard experiment to the detection of exotic processes

Aldo Morselli

*Dipartimento di Fisica dell'Università di Roma "Tor Vergata"
and INFN Sezione di Roma 2
Via della Ricerca Scientifica 1 , 00133 Roma, (Italy)*

Paper presented at the Workshop "The dark side of the Universe"
Roma, 23-25/6/93

Abstract

The direct detection of primary cosmic rays is a difficult task because must be carried out with particle detectors outside the atmosphere, i.e. on balloons or satellites, but it offer unique possibility to study the spectrum and the isotopic composition of cosmic rays, that are essential to understand the origin and the dynamic evolution of the matter in the galaxies. The direct detection of annihilation products in cosmic rays offer also an alternative way to search for dark matter particles candidates. Here we will see in particular that the study of the spectrum of antiproton, positrons and gammas offer good possibilities to perform this search and we will review our experimental effort in this direction.

1 Antiprotons

Figure 1 summarized the experimental and theoretical situation in the study of the antiproton flux compared with the proton flux. A certain amount of antiproton can be produced through the interaction of the cosmic rays with the interstellar matter and we can know how much it is applying the standard scheme of cosmic ray propagation models which compute the expected \bar{p} flux starting from the proton flux, the antiproton production cross - section and the quantity of traversed matter (line called *standard leaky box* in figure 1) [1]. One feature that one can see from the figure is that the observed flux appears to be 3 times higher than the expected. The over-abundance of antiprotons has led to speculations of their origin (for a review see [2] or [3]) ranging from models were the antiprotons are produced in shrouded supernova [4] to more exotic ones. For example, the model called *antigalaxies* comes from the consideration that the role of antimatter in the creation of the universe is still not clear and at this moment can not be ruled out the hypothesis of the presence in some part of the universe of a certain amount of antimatter [10]. In only this case the ratio

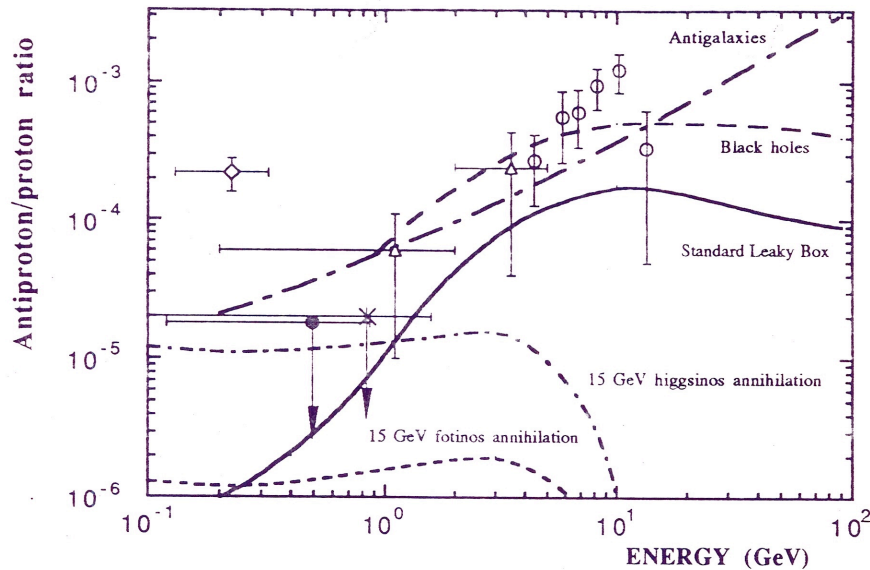


Figure 1: The experimental points are shown compared with the different models for the antiproton/proton ratio as explained in the text. The experimental points are: \circ Golden et al. [5], \triangle Bogolomov et al. [6], \diamond Buffington et al. [7], \times Ahlen et al. [8], \bullet Streitmatter et al. [9]

\bar{p}/p is expected to rise with the increase in energy just because the extragalactic component of the cosmic rays increase with energy.

Another possible process for generating antiprotons is the spontaneous emission of proton- antiproton pairs near small black holes [11]. These might be primordial or remnants of the Big Bang from which the Universe evolved; their evaporation can give a contribution to the antiproton production (line called *black holes* in figure 1).

But the more interesting hypothesis for what concern the study of the dark matter is the possibility that the excess of antiprotons comes from the annihilation of supersymmetric particles [12].

These particles can be or photinos ($\tilde{\gamma}$) or their generalized extension to neutralinos, including higgsinos, (\tilde{h}) that were shown to be cosmologically significant by Goldberg [13] and Ellis et al. [14] respectively. The photino annihilation results in antiproton spectra with a cut-off at an energy corresponding to the supersymmetric particles mass. As can be see from figure 1, the calculations show that it may be possible to look for a dark matter halo annihilation signal at \bar{p} energies below 1 GeV, where the flux from cosmic-ray collisions is expected to be negligible.

The \bar{p} spectra was calculated using the Lund Monte Carlo Program [20] that takes in account the different fragmentation effects associated with heavy quark jets and provide a framework for extrapolating from collider data to a different

mixture of final state quark jets. The reason of the difference between the $\tilde{\gamma}$ and the \tilde{h} is that the τ production, that is unimportant in $\tilde{h}\tilde{h}$ annihilations, accounts for 56% of $\tilde{\gamma}\tilde{\gamma}$ annihilations and produces no \bar{p} . For what concerns baryon formation the Lund model uses a diquark-quark mechanism for baryon production and may, for certain situations, predict a \bar{p} production rate which is a factor two too low, but on the other hand seem that it may overestimate the flux of high energy proton by a factor two [21]. Due to this uncertainties the present upper limits in the low energy range do not constrain any astrophysical parameters for all the χ particles of interest but it is possible to hunt for χ 's with low energy \bar{p} experiment at a flux level not too far below the present upper limits.

2 Positrons

The positrons (like the electrons) are an unique probe of the acceleration mechanisms in the sources, of distribution of acceleration sites and of interactions in interstellar space, because of their low rest mass and because (contrarily to nucleons which, at high energies, suffer attenuation due to collisions with gas) they interact with nuclei fields by bremsstrahlung, with photons by inverse Compton scattering and with magnetic fields through synchrotron radiation.

In figure 2 is shown the experimental situation and the predictions of two standard cosmic ray propagation models [22] (Standard Leaky Box and Dynamical Halo); one can see that there is a unexplained increase in the positron fraction for energies greater than 10 *GeV*.

A way to explain this increase was proposed by Tilka [23], that has observed that the annihilation of a massive weakly interacting massive particles (WIMP, hereafter referred to as χ) with $M_\chi \geq 20$ *GeV* and with a large cross section for producing a single e^+e^- pair, can account for the extra positrons. A clear way to test this model will be to look at higher energies because a prediction is that these annihilations would yield a sharp break in the cosmic ray positron at energy equal to M_χ . It must be noticed that only massive Dirac neutrinos (ν_D) generate such a feature. The reason why the neutralinos cannot be the responsible for the excess of e^+ is the small branching ratio of the channel $\chi\chi \rightarrow e^+e^-$ that is the order of 10^{-5} in the simplest supersymmetric model; in other words they will produce much more \bar{p} than e^+ and in this case their number is constrained by the \bar{p} flux data, although it may be possible to enhance $B(\chi\chi \rightarrow e^+e^-)$ in more complicated supersymmetric models.

As can be seen from figure 2, the shape of the $e^+/(e^+ + e^-)$ ratio depends critically on the containment time τ of the electrons in the halo. The value $\tau = \tau_8 \cdot 10^8$ *yr* may be estimated from studies of cosmic ray nuclei; in particular the abundance [24] of the radioactive nuclide ^{10}Be and stable secondary nuclei suggest $\tau_8 \sim 0.1$ if cosmic rays are confined to the galactic disk or $\tau_8 \sim 1$ if they diffuse through a halo of radius ~ 10 *kpc*.

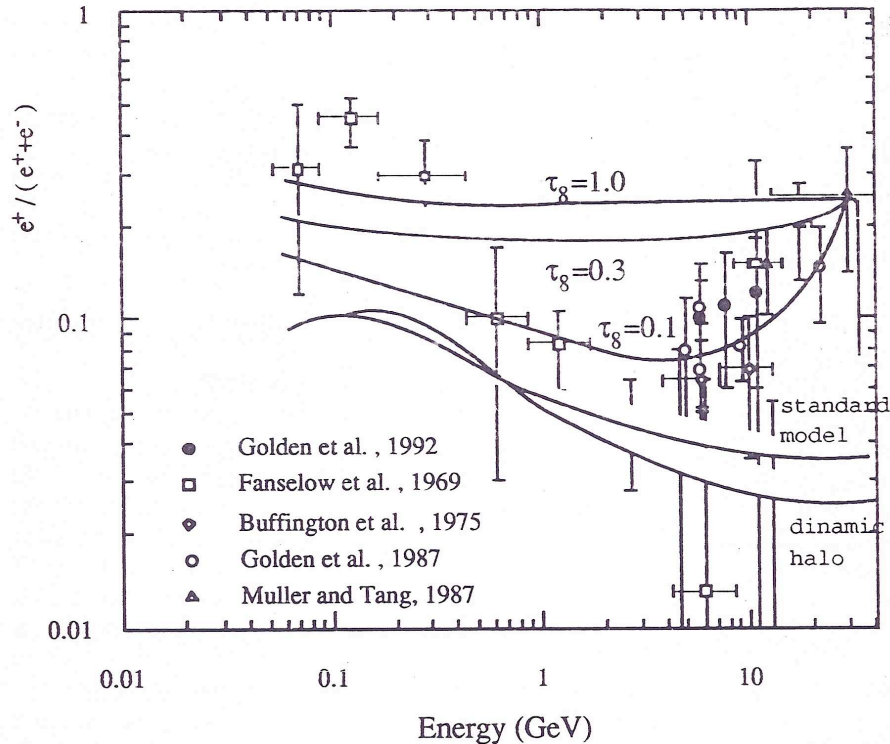


Figure 2: Measurements of the positrons to total electrons ratio are compared with predictions of two standard cosmic ray propagation models (Leaky Box and Dynamical Halo) and with the Dirac Neutrino model for three values of τ_8 as explained in the text. The experimental points are: Golden et al. 1992 [15] Fanselow et al. , 1969 [16] Buffington et al. , 1975 [17] Golden et al., 1987 [18] Muller and Tang , 1987 [19]

3 Experimental Program

As we have seen in the previous two sections precise measurements of the anti-proton and positron spectra in a large energy range (at least between 0.3 and 50 GeV) are needed to tell if the exotic particles annihilation play a role. Our experimental effort in this direction has already begin with the MASS apparatus, shown in figure 3. The payload has flown on a balloon twice, the first flight took place from Prince Albert, Sask. on Sept 5 , 1989. This flight lasted only 5.5 hr. due to an unfavorable wind speed and direction, but any way produced the data called Golden et al. 1992 in figure 2. A second flight took place from Fort Sumner, New Mexico, on Sept 1991 for 9 hr. and the data are under analysis.

The main parts of the apparatus, are : a) the tracking system, that consist of 8 multi-wire proportional counter (MWPC) and two drift chamber each containing 10 layers of hexagonal drift cells (the drift chamber modules were

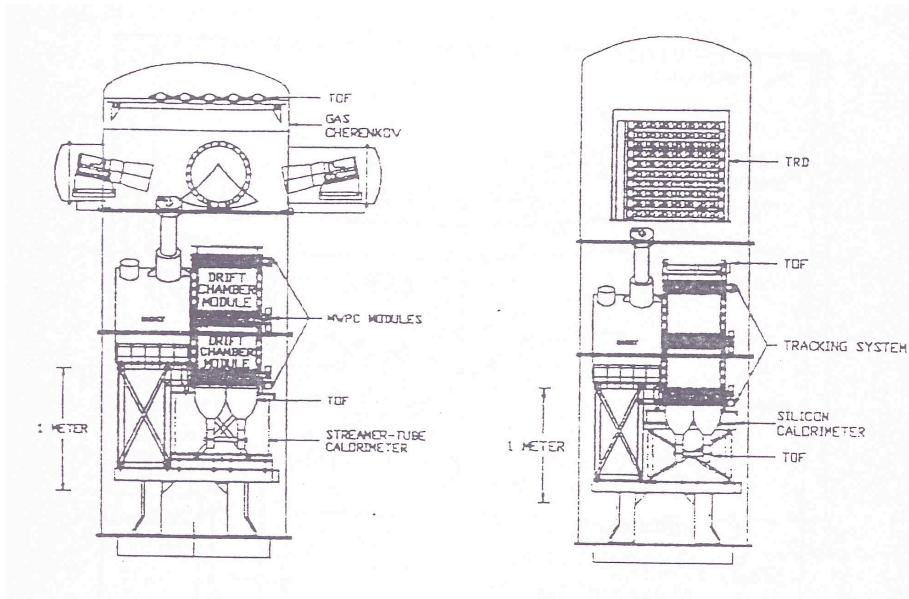


Figure 3: The MASS (left) and the TRAMP-Si (right) configurations of the balloon payload

added after the 1989 flight). Both system have spatial resolution better than $200 \mu m$. Details of the MPWC system can be found in Golden et. al. [25] b) a Cerenkov detector with a path length of $1 m$ of Freon 12 viewed by four photo tubes. A 4-section pyramidal mirror (each segment being a paraboloid) is used to focus the light on the photo tubes. A fully relativistic particles typically produces 14 photo - electrons and the efficiency for detection of a muon above the threshold γ_{tr} is 98%, while the accidental rate is less then $5 \cdot 10^{-4}$ for low energy muons. c) the time of flight (TOF) scintillators are used to determine the direction of travel. They are also pulse-height analyzed in order to determine the magnitude of each particle's charge. The TOF time resolution is about $200 ps$ and since the top and bottom TOF layer are separated by $1.2 m$, the time difference between downward and upward particles is at least 30 std.dev.. d) the calorimeter consist of 40 layers (20 in each of two orthogonal view) of 64 brass streamer tubes for a total of 7.3 radiation length of brass [26] . The special feature of the calorimeter is that it provide not only an energy resolution, but also an accurate reconstruction of the annihilation vertex and of the out coming tracks. This is particularly useful to discriminate between electromagnetic and hadronic particles in a situation where the total containment of the particle is forbidden by the weight limitation of the payload.

The MASS configuration is limited to about $20 GeV$ in the highest energy for positron observation because as the proton Cerenkov threshold is reached we expect increasing background. In order to eliminate this undesirable characteristic a transition radiation detector(TRD) is being used in the 1993 flight

series (Tramp-SI) for the observation of high energy positrons. The TRD uses precisely carbon fibers to provide transition in refractive index. An extremely relativistic ($\gamma > 1000$) particle traversing these transition will emit x-rays of an energy that can be detected by an MWPC. Electrons and positrons with energies above 500 *MeV* satisfy this criterion but protons must have an energy above 1 *TeV* to produce transition radiation. The TRD consist of 11 layers of carbon fibers each separated by a MWPC. This allow good efficiency , redundancy and detector cross-checks. Details of the TRD design and test results may be found in [27] where one can see that with an efficiency of 90% for the detection of positrons, the TRD can falsely identify $4 \cdot 10^{-4}$ of the proton as positrons . Positrons are especially difficult to identify because the e^+/p ratio is on the order of 10^{-3} at low energy decreasing to 10^{-4} at high energies. Thus to measure positrons reliably, one would like to have a system which has a probability of misidentifying a proton as a positron which is 10^{-5} or better. To accomplish this a silicon imaging calorimeter is used in connection with the TRD. The silicon calorimeter offers significant improvement over the MASS streamer tube calorimeter in two areas : 1) it gives energy position in each strip rather than "on / off" indication and this allow precise determination of the longitudinal and lateral profile of the shower and 2) decreased vertical height, thus allowing a greater geometrical factor. In the Tramp-SI configuration the calorimeter is formed by 5 layer of silicon detector alternated with 1 radiation length of tungsten. A single layer is composed as a $8 \cdot 8$ matrix of sensitive modules (see figure 4) and each modules is formed by two silicon detectors, each having a total area of $6 \times 6 \text{ cm}^2$ and a thickness of 380 μm ; they are mounted back to back with perpendicular strips to give x and y coordinates. Each module has 16 strips 3.6 *mm* wide connected to the neighboring one to form single strips 50 *cm* long. Details of the silicon calorimeter design and test results may be found in [28]

The silicon calorimeter in this 5 plane configuration will provide a factor $2 \cdot 10^{-3}$ in rejection power that, combined with the TRD, give us an overall error rate for proton misidentified as positrons better than $8 \cdot 10^{-7}$. This instrument has already flown in September 93 for a total data taking time of 24 hours.

The very low energy part of the positron and antiproton spectrum (below 5 *GeV*) remains uncovered by the previous program and then we are planning a flight dedicated to this items for the summer of 1994 (CAPRICE flight). A ring imaging Cerenkov detector (RICH) with the TOF system, the tracking system and the silicon calorimeter will be used. The radiator of the RICH is 1 *cm* of *NaF* (refractive index=1.4). This is followed by a helium-filled space which allow the expansion of the Cerenkov disk and the formation of a ring of Cerenkov photons. The Cerenkov ring is then transmitted through a quartz window into an MWPC filled with methane, isobutane and TMAE (tetra-dimethyl-amine-ethylene). The MWPC utilizes a segmented cathode readout (8 *mm* squares) to record $x - y$ location of the particle passage and the conversion location for the Cerenkov photons. Details of the design can be found in ref.[29] . The performance of a prototype system has been measured in a series of test runs

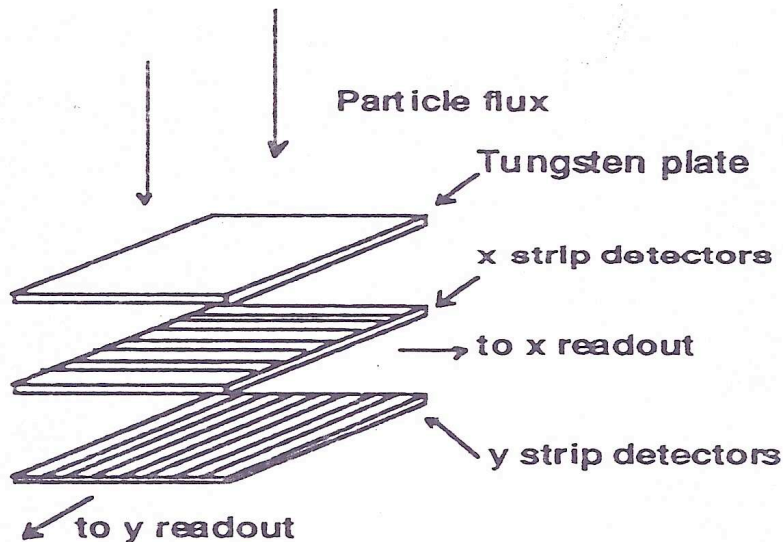


Figure 4: The basic module of the calorimeter

at CERN.

In the energy range 1-4 GeV the Cerenkov ring diameters of e^- and μ^- are more than 10 std.dev. from that of the antiproton, consequently the separation of the background from antiprotons is assured using only the Rich. Above 4 GeV the ring diameters begin to converge, but at these energies the calorimeter has excellent rejection power against the electrons. The e^+ and e^- will be separated from the μ with the request of electromagnetic cascade in the calorimeter.

Table 1 summarize our experimental program and one can see that extension of the energy range can only be obtained with long duration flights (> 10 days) or with a satellite. Long duration flights are under study because will require attention to a number of aspects of payload design: 1) power 2) weight, 3) thermal control 4) recording 5) magnet lifetime. They are really competitive only if there is no possibilities in a short time (before the 2000) of a satellite. The Wizard mission [30] on the Space Station, already approved, is delayed due to the general delayed of the Space Station program. There are now studies both with NASA and Russian agencies to modify the Wizard project to make it suitable for a rocket launch.

4 Photons

The annihilation of supersymmetric particles can produce also photons. For example in ref.[31] is shown that the gravitino can be a dark matter particle if the second lightest supersymmetric particle is the sneutrino. The gravitino can

decay due to R-parity violation processes. The most stringent lower limit on the gravitino lifetime is imposed by the diffuse gamma-ray flux and the positron flux. The two particle decay of the gravitino $G \rightarrow \nu + X$ and $G \rightarrow \gamma + X$ can produce a detectable gamma line and a marginally detectable neutrino line. Let consider first the diffuse gamma radiation. The present day Universe, $t = t_0$ is transparent for photons borne in decays of the gravitino. Decay electrons are breaking on relic 2.7 K black-body radiation producing isotropic gamma radiation with a spectrum

$$I_\gamma(E_\gamma) = \frac{c}{8\pi} r_{em} \frac{t_0}{\tau_G} \rho_c \epsilon_X^{-1/2} E_\gamma^{-3/2}$$

where $\rho_c = 1.06 \cdot 10^{-29} h_{75}^2 g/cm^2$ ($h_{75} = H_0/75 km s^{-1} Mpc^{-1}$ and H_0 is the Hubble constant), τ_G is the gravitino lifetime, r_{em} is the product of the branching ratio for the decay of the process $\tilde{\nu} \rightarrow G + \nu + e^+ + e^-$ ($\simeq (\alpha/\pi)^2$) and the fraction of the energy transferred to the $e^+ + e^-$ pair (~ 0.5), ϵ_X is the maximum energy of the spectrum ($\simeq 3.6 m_{100} MeV$) and m_{100} is the gravitino mass normalized at 100 GeV.

A line with such an intensity at energy $E_\gamma \sim 50 m_{100}$ can be discovered with detectors tuned for high gamma energy ($> 10 GeV$) with good energy and angular resolutions to discriminate better the discrete sources from the diffuse background.

Only a satellite bigger than EGRET [32] can accomplish these results. A possible solution that we are studying is to use the silicon calorimeter surrounded with anticoincidence shields. A configuration with 20 planes $50 \cdot 50 cm^2$ interleaved with 0.5 X_0 of Tungsten is very compact (about 30cm in height) and then has a large geometric factor and can collect a large statistics. From preliminary study it has a good energy resolution (10% at 10 GeV) that decrease at high energies and a good angular resolution ($\sim 0.5^\circ$ at 10 GeV). The relatively low weight of this kind of detector ($\sim 400 \div 500 Kg$) make it suitable for a flight together with other instruments in a Resource-0 Russian satellite to be flight before 2000.

References

- [1] T.K. Gaisser and B.G. Mauger , Phys.Lett. , 30 , 1973 , 1264.
- [2] S.A. Stephens and R.L. Golden , Sp. Sci. Rev. , 46 , 1987 , 31.
- [3] G. Basini, A. Morselli , M.Ricci , Riv. Nuovo Cimento , 12 , 1989 , 4.
- [4] S.A. Stephens and B.G. Mauger , Ap. Sp. Sci , 110 , 1985 , 337.
- [5] R.Golden et al. , Astr. Lett ,24 ,1984 ,75.
- [6] E.A.Bogolomov et al. ,XX ICRC Moscow ,2 ,1987 ,72.
- [7] A. Buffington et al. , Ap.J. ,248 ,1981 ,1179.

- [8] S.P. Ahlen et al. ,*Phys.Rev.Lett* ,61 ,1988 ,145.
- [9] R.E.Streitmatter et al. , XXI ICRC Adelaide , 3 , 1990 , 277.
- [10] R.W. Brown and F.W. Stecker , *Phys.Rev.Lett.*, **43** , (1979), 315.
G.Senjanovic and F.W.Stecker , *Phys.Lett.*, **96B**, (1980), 285.
K.Sato , *Phys.Lett.* , **99B** , (1981) , 66.
F.W.Stecker , *Nuc.Phys.*,**B252**, (1985) , 25.
- [11] P.Kiraly et. al. , *Nature* , 293 ,1981 ,120.
- [12] J. Silk and M.Srednicki ,*Phys.Rev.Lett.* ,53 ,1984 ,624.
F.W.Stecker,S.Rudaz and T.F.Walsh ,*Phys.Rev.Lett.* ,35 ,1985 ,1.
F.W.Stecker and A.J.Tylka , *Astr.J.* ,336 ,1989 ,L51.
- [13] H.Goldberg , *Phys.Rev.Lett* , 50 ,1983 ,1419.
- [14] J. Ellis et al. , *Nucl.Phys.* , B238 ,1984 ,453.
- [15] Golden et al. XXII ICRC Dublin , OG 7.1.1,1991 , LNF-92-052 (P), 1992.
- [16] J.L.Fanselow et al. , *Ap.J.* , 158 ,1969 , 771.
- [17] A.Buffington et al. , *Ap.J.* ,199 ,1975 , 669.
- [18] R.L.Golden et al. , *Ap.J.* , 287 ,1987 , 622.
- [19] D.Muller and K.K.Tang ,*Ap.J.* ,312 , 1987 , 183.
- [20] T. Sjostrand , *Comp.Phys.Comm.* , 39 , 1986 , 347.
- [21] sh G.D..Cowan, Ph.D. thesis, LBL-247115.
- [22] R.J.Protheroe , *Ast.J.* , 254 ,1982 , 391.
- [23] A. J. Tilka , *Phys. Rev. Lett.* , 63 , 1989 , 840.
- [24] M.E. Wiedenbeck and D.E. Greiner , *Astr. J.* ,239 ,1980 ,L139.
- [25] R. Golden et al. ,*Nucl. Inst. and Met.* , A206 ,1991 , 366.
- [26] G.Basini et al. ,*Il Nuovo Cimento* ,11C ,1988 , 339.
- [27] E.Barbarito et al. , *Nucl.Ins. and Meth.* , A313 , 192 , 296.
- [28] M.Bocciolini et al. , *Nucl.Phys.B* , 32 ,1993 ,77.
G.Barbiellini et al., INFN-AE 92-17.
- [29] T.Francke, F.Suffert , *NIM* , A283 ,1989 , 608.
- [30] R.L Golden et al. ,*Il Nuovo Cimento* ,105B ,1990 , 191.
- [31] V.S. Berezinsky ,*Phys.Lett.B* ,261 ,1991 , 71.
- [32] R.C. Hartman et al. , *Ap.J.* , 385 ,1992 , L1.